Technical Reports on Frostwing Flat Plate CFD Simulations

Pekka Koivisto, Tomi Honkanen

Trafi Research Reports
Trafin tutkimuksia
Trafis undersökningsrapporter
7/2017

Trafi Finnish Transport Safety Agency

Date
31.3.2017

Title of publication
Technical Reports on Frostwing Flat Plate CFD Simulations

Author(s)
Pekka Koivisto, Tomi Honkanen

Commissioned by, date
Kari Wihlman, August 26th 2016

Publication series and number
Trafi Research Reports 07/2017

ISSN (online) 2342-0294
ISBN (online) 978-952-311-196-7
URN http://urn.fi/URN:ISBN:978-952-311-196-7

Keywords
CFD, aircraft, aerodynamics, anti-icing fluids

Contact person
Erkki Soinne

Language of the report
English

Abstract
This research report summaries the flat plate CFD simulation work done as part of the second year of the Frostwing project. The contents have previously been reported as three separate technical memorandums.

The first chapter covers the investigation on the effect of the air density on the fluid flow-off. The CFD investigation began before the wind tunnel flat plate tests were planned and hence the fluid properties have been slightly different in the simulations done previously.

In the second chapter the study on the effect of the acceleration of the air inflow velocity ramp is presented. A new inflow acceleration profile (velocity ramp) was generated with the data obtained from the wind tunnel tests. The results of the simulation with the new ramp are compared to the results of the past simulations.

The main effort in the CFD work has been on the simulation of the behavior of Type I deicing fluid, which is a Newtonian fluid. At the beginning of the previous Icewing project there was a brief effort to simulate non-Newtonian Type IV anti-icing fluids, but this proved to be challenging. In the second year of the Frostwing project, it was decided that more effort will be put on this subject. This preliminary investigation led into better understanding of the challenges related to non-Newtonian simulations with OpenFOAM software. The findings are reported in the third chapter.

FOREWORD

This research report documents findings of the CFD simulations of de/anti-icing fluid behavior on a flat plate in an airstream over it. It forms part of the second year of the Frostwing project, performed under a Research agreement between the Federal Aviation Administration FAA and the Finnish Transport safety Agency Trafi together with the National Aviation and Space Administration NASA, on the research of frost and anti/de-icing fluid effects on aircraft wing at take-off.

The research was done by the team of Arteform Oy, headed by MSc Juha Kivekäs.

Helsinki, March 31st 2017

Erkki Soinne

Chief Adviser, Aeronautics

Finnish Transport Safety Agency, Trafi

Index

Nomenclature

k	constant, power-law coeffcient	
n	power-law coefficient	
p	constant	
S	shear rate	
t	time	
U_{init}	initial velocity	
U_{ref}	reference velocity	
U_{∞}	inflow velocity	
$v_{i,j,k}$	velocity components	
x, y, z	coordinates	
ρ	density	
μ	dynamic viscosity	note units: N·s/m^2 = kg/(m·s) = Pa·s = 1000 cP
ν	kinematic viscosity (μ/ρ)	note units: m^2/s

1 The effect of the air density on the flat plate CFD results

The preliminary Icewing CFD Investigation (ref. [3]Koivisto and Auvinen) on de/anti-icing fluid flow on a flat plate with an accelerating airflow over it was a trial and error based effort in order to assess the possibilities of such simulations. As a simplification, an air density of 1.0 kg/m^3 was used in all the preliminary simulations. This was also used in the grid resolution and parameter sensitivity study (ref. [4]Koivisto and Honkanen) in order to compare the results with the preliminary simulations. At this point wind tunnel test data from the flat plate experiments was already available with air density being typically over 1.2 kg/m^3.

In order to compare the CFD simulation results with the results of the wind tunnel tests in the future, it was decided that a simulation with comparable air density must be done. The effect of the fluid viscosity was also included in this check. The effect of the different air acceleration profile in the simulations and the wind tunnel tests remains to be investigated separately.

1.1 Fluid properties

Case C2 from ref. [4]Koivisto was selected as a reference case. Two new simulations, Case_RHO and Case_NU, were run to check the effect of the air density and fluid viscosity. The same grid with the same boundary conditions were used as in case C2.

Case C2 = original 160k grid, new trailing edge outlet BC for the phase fraction variable α

Air density	ρ_{air}	1.0 kg/m^3
Liquid density	ρ_{liquid}	1040 kg/m^3
Air kinematic viscosity	ν_{air}	1.48 x 10^{-5} m^2/s
Liquid kinematic viscosity	ν_{liquid}	2.0 x 10^{-5} m^2/s

Case_RHO

Air density	ρ_{air}	1.2 kg/m^3
Liquid density	ρ_{liquid}	1040 kg/m^3
Air kinematic viscosity	ν_{air}	1.48 x 10^{-5} m^2/s
Liquid kinematic viscosity	ν_{liquid}	2.0 x 10^{-5} m^2/s

Case_NU

Air density	ρ_{air}	1.0 kg/m^3
Liquid density	ρ_{liquid}	1040 kg/m^3
Air kinematic viscosity	ν_{air}	1.48 x 10^{-5} m^2/s
Liquid kinematic viscosity	ν_{liquid}	3.0 x 10^{-5} m^2/s

1.2 Results

The results reveal that both air density and liquid viscosity have an effect on the total liquid volume on the flat plate and the rate of the liquid flow-off. The total liquid volume over the simulated time is shown in Figure 1. The increase of the liquid viscosity from 2.0 x 10^{-5} to 3.0 x 10^{-5} m^2/s slows the liquid flow and results in approximately 8 percentage points more liquid remaining at t = 5 s. The increase of the air density does not affect the rate of the liquid removal but the removal begins earlier at t = 1.5 s and therefore the remaining volume is about 9 percentage points less than the reference at t = 5 s. These differences are shown in Figure 2 and Figure 3.

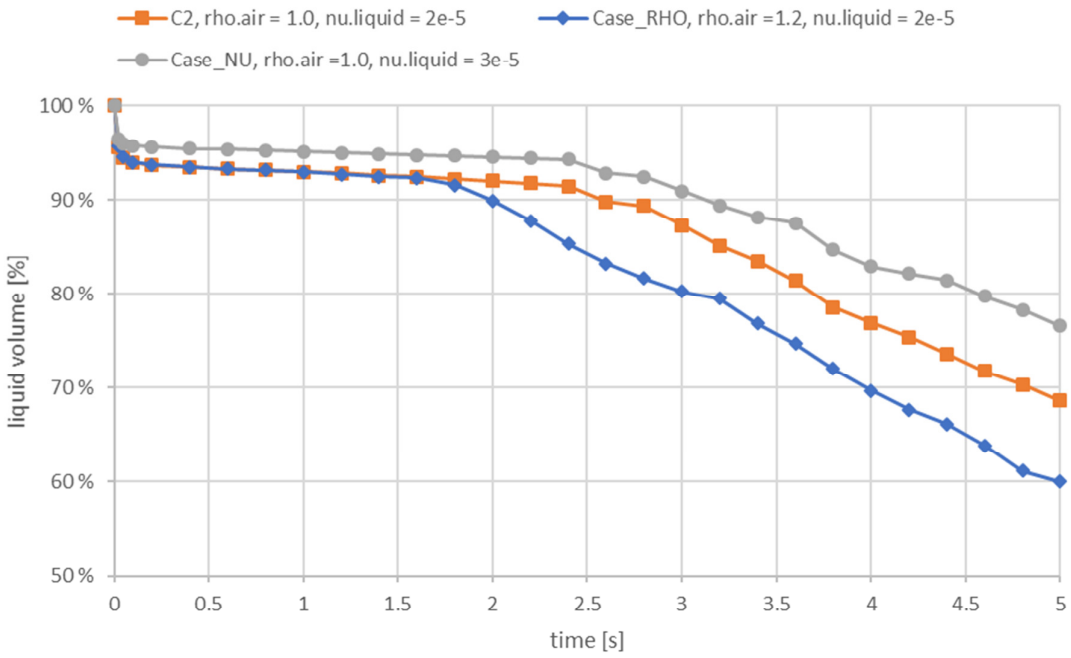

Figure 1. Total liquid volume % on the flat plate over time.

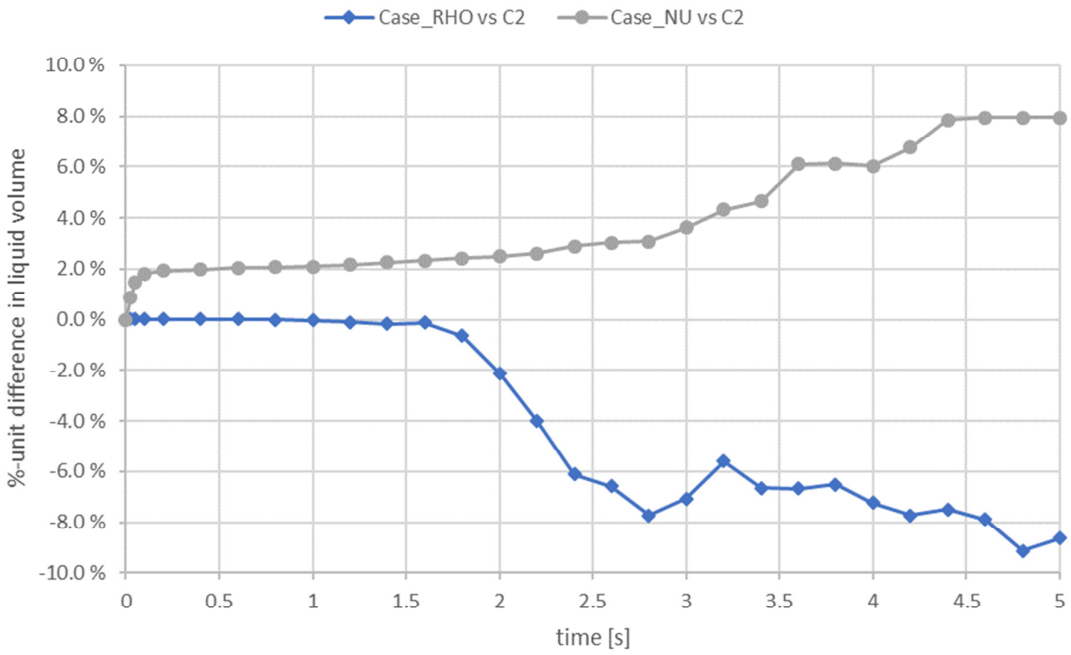

Figure 2. Difference in liquid volume % compared to case C2.

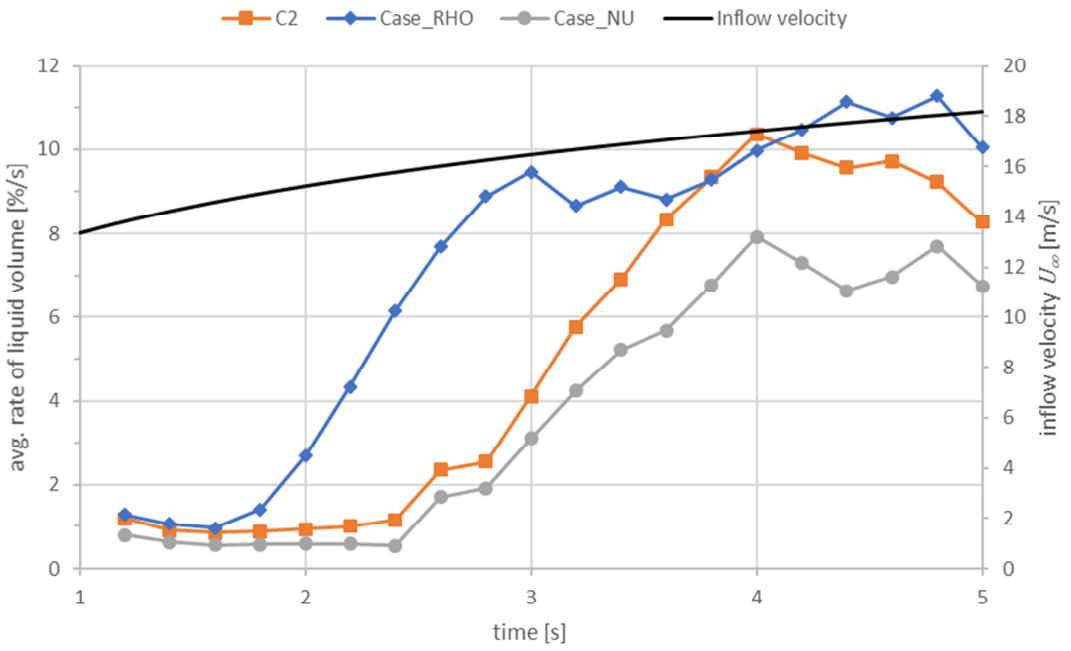

Figure 3. Liquid volume flow rate %/s averaged over 1 second (moving average).

The results were also compared with the results from a wind tunnel experiment with air density $\rho_{air,W/T}$ = 1.231 kg/m^3 and liquid kinematic viscosity $\nu_{liquid,W/T}$ = 3.365 x 10^{-5} m^2/s (35 cP). The simulations results were fitted to the wind tunnel results with a timeshift method by matching dynamic pressure q_∞ as well as possible. It was discovered that the results from Case_RHO required an additional timeshift of +0.5 seconds to better match the wind tunnel dynamic pressure and this also resulted in better match to the flow-off results in reference case C2. This is seen in Figure 4 and Figure 5.

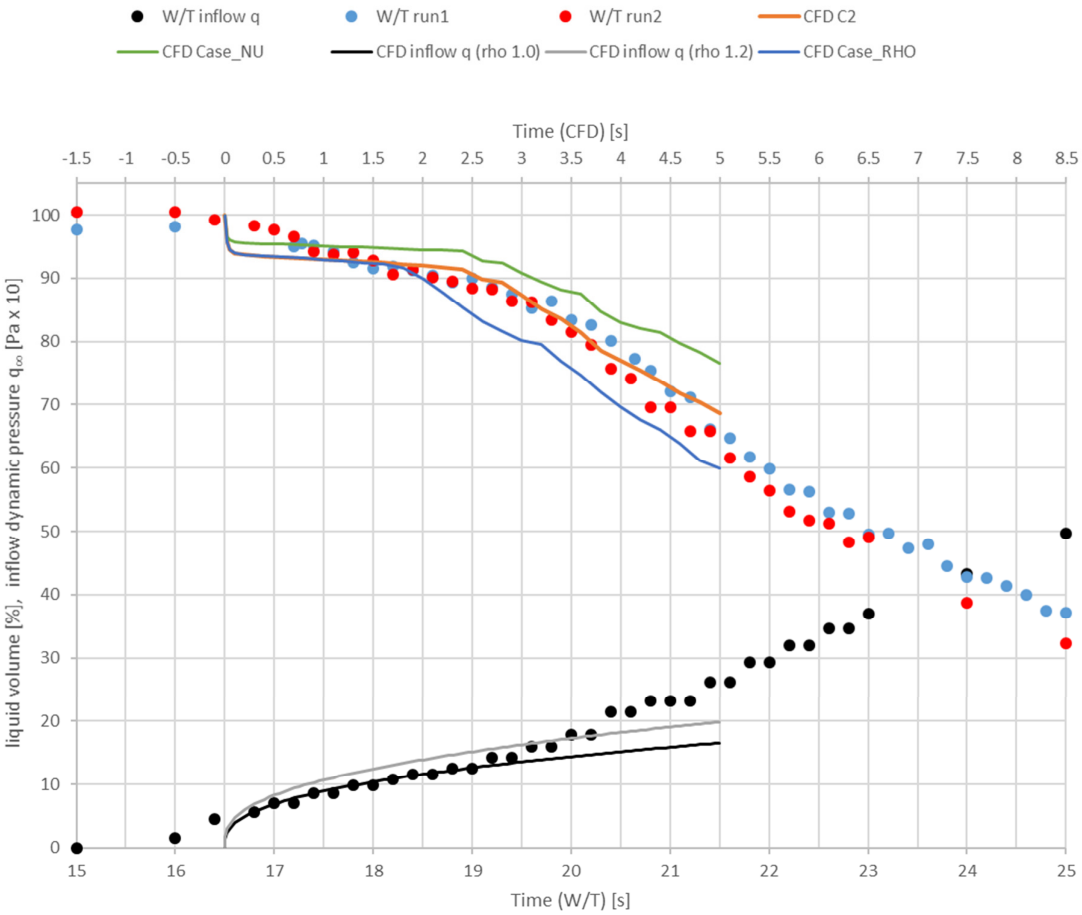

Figure 4. Comparison of the simulation results to the wind tunnel results using the inflow dynamic pressure and timeshift method. $\boldsymbol{\rho_{air,W/T}}$ = 1.231 kg/m^3 and $\boldsymbol{\nu_{liquid,W/T}}$ = 3.365 x 10^{-5} m^2/s (35 cP).

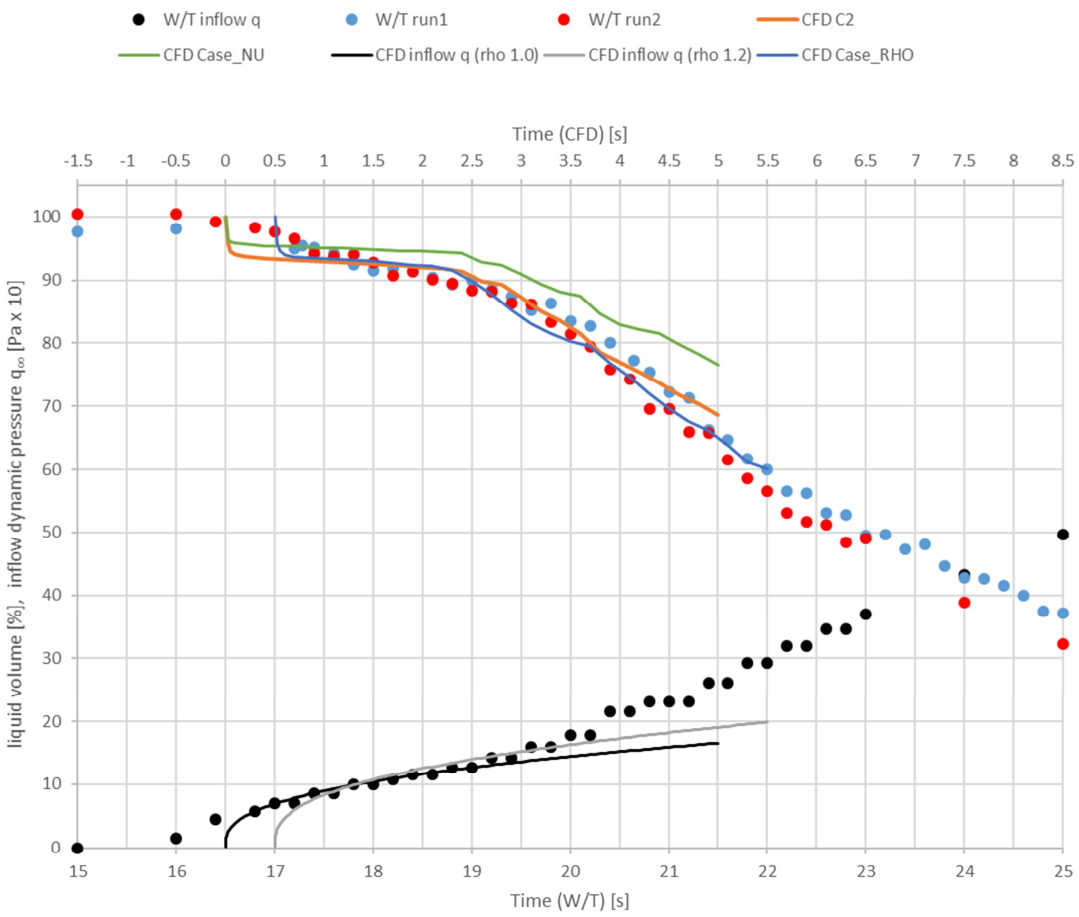

Figure 5. Comparison of the simulation results to the wind tunnel results. CFD Case_RHO and corresponding CFD inflow q (rho 1.2) timeshifted +0.5 s in order to achieve better match to W/T inflow q. CFD Case_RHO and C2 results also show better match.

1.3 Conclusions

The following conclusions can be made from the results:

- Both properties ρ_{air} and ν_{liquid} have an effect on the results
- Increasing the viscosity of the fluid ν_{liquid} slows the action which is a logical consequence
- Increasing the air density ρ_{air} leads to the removal process starting earlier but the effect on the removal rate is negligible. Over the long term as the liquid layer gets thinner and wave height lower the difference between total volume seems to stabilize at approximately 8 %.
- A good match to the wind tunnel results is achieved with additional +0.5 s timeshift
- The findings support the assumption that the flow-off phenomenon is driven by the dynamic pressure of the air

2 Comparison of air inflow velocity ramps and their effect on fluid removal over time

The CFD research of de/anti-icing fluid flow on a flat plate was started as a part of the Icewing project before any flat plate tests were done in the wind tunnel (ref. [3]Koivisto). The non-linear acceleration of the incoming airflow in the simulations was therefore selected based on requirements of computational time, not on any validation data. Later a couple of simulations were run with linear acceleration with the presumption that it would better replicate the wind tunnel test conditions. These simulations required more computational time due to the slower acceleration compared to the simulations with the non-linear velocity ramp.

The wind tunnel flat plate tests have now been analyzed and with the available data a new inflow air velocity ramp was generated by fitting a polynomial curve to the wind tunnel speed measurements. A new simulation has been done with this new inflow acceleration profile. The results are compared to the those of the original non-linear ramp and the linear ramp. Two previous cases with matching air and fluid properties were selected for this purpose.

2.1 Velocity ramps used in the simulations

The new velocity ramp was generated by modifying two constants in the polynomial of the original non-linear ramp. The polynomial is shown in equation (1) and the constants in Table 1.

$$U_\infty(t) = U_{ref} k t^p + U_{init} \quad (1)$$

Table 1. Inflow velocity ramp polynomial constants.

Constant	Original non-linear	Wind tunnel fit
U_{ref}	15	15
k	1/1.32	1/3.3
p	0.22	0.775
U_{init}	2	2

The new velocity ramp is shown with the wind tunnel speed measurements used in the fitting in Figure 6. The curve fitting was done manually with emphasis in earlier time instants. In later time instants the acceleration and the velocity of the simulations slightly lag the wind tunnel measurements. Another constraint was the initial velocity of 2 m/s that was decided to be kept the same in as in previous simulations. The wind tunnel data is anyways quite inaccurate when the wind tunnel fan starts to accelerate from idle speed.

The original and the new, wind tunnel data fitted, velocity ramps are shown in Figure 7. The linear 2 m/s^2 acceleration ramp is also shown. The initial velocity is 2 m/s. The original non-linear ramp is clearly more aggressive at the beginning, but settles down later while the other two ramps continue accelerating at approximately 2 m/s^2.

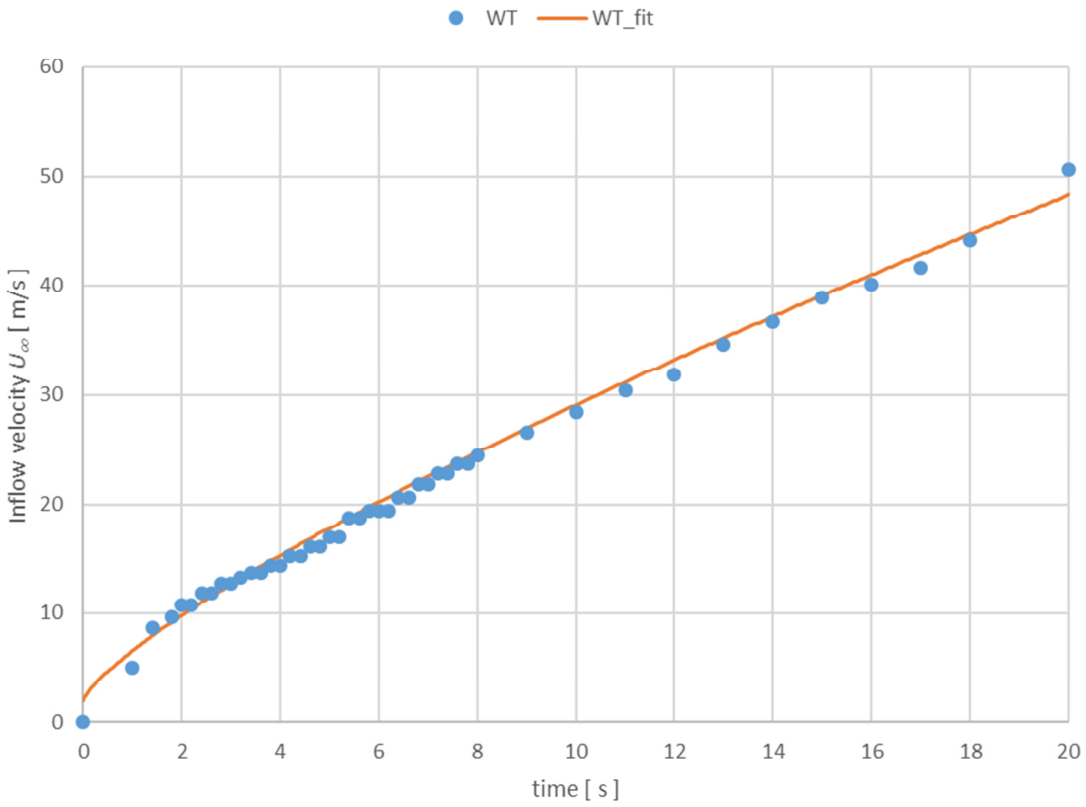

Figure 6. The new CFD inflow velocity ramp fit to the wind tunnel speed measurements.

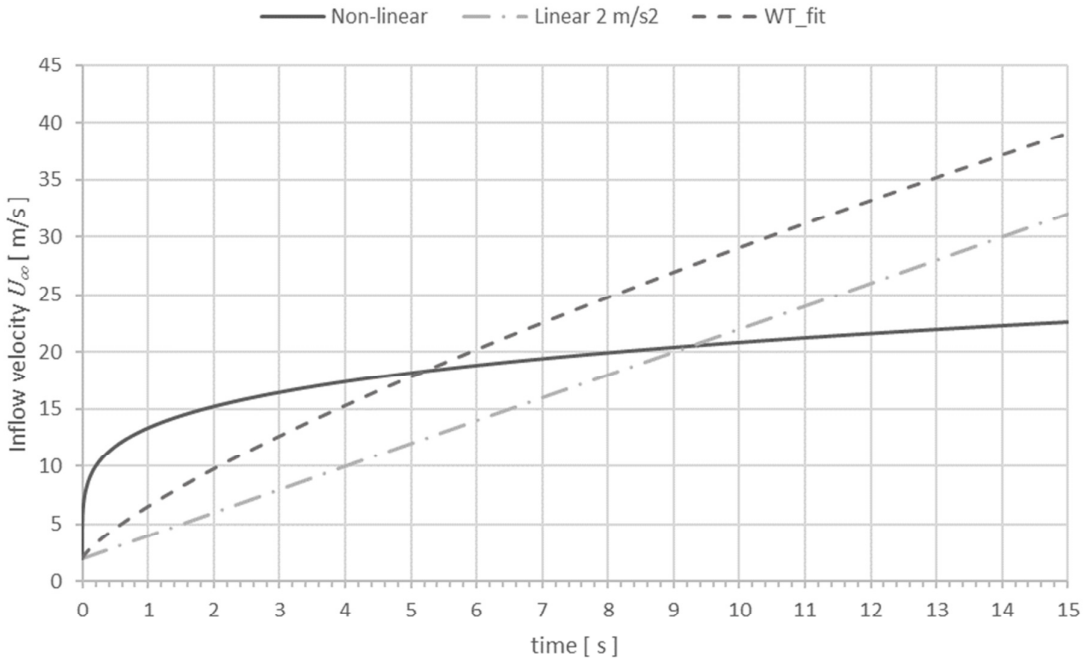

Figure 7. Comparison of the velocity ramps used as inflow boundary condition in the CFD simulations.

2.2 Description of the simulation cases

Two previous cases were selected for comparison: case P4 from the preliminary simulation series (ref. [2]Honkanen) with the linear acceleration, and case NU from the air density and liquid viscosity effect study (ref. [1]Honkanen and Koivisto) with the original non-linear velocity ramp. In these cases the fluid properties were ρ_{air} = 1.0 kg/m^3, ν_{air} = 1.48 x 10^{-5} m^2/s, ρ_{liquid} = 1040 kg/m^3, and ν_{liquid} = 3.0 x 10^{-5} m^2/s. Case P4 has been simulated for 14 seconds of simulated time. In order to compare the differences in liquid volume due to the inflow velocity effect, the case NU was simulated further from 5 seconds until 8 seconds (the fluid removal begins later in case P4). The new velocity ramp case WT_fit was also simulated for 8 seconds. In all the cases the initial liquid layer thickness is 1 mm.

2.3 Results

Comparison of the total liquid volume on the flat plate over time is shown in Figure 8. The results are in agreement with the expectations based on the velocity ramps. The non-linear ramp is the most aggressive at the beginning followed by the wind tunnel fit. For the linear case P4 the removal begins later at t = 5.2 seconds. As the acceleration of the non-linear ramp slows down, the other two continue at constant 2 m/s^2.

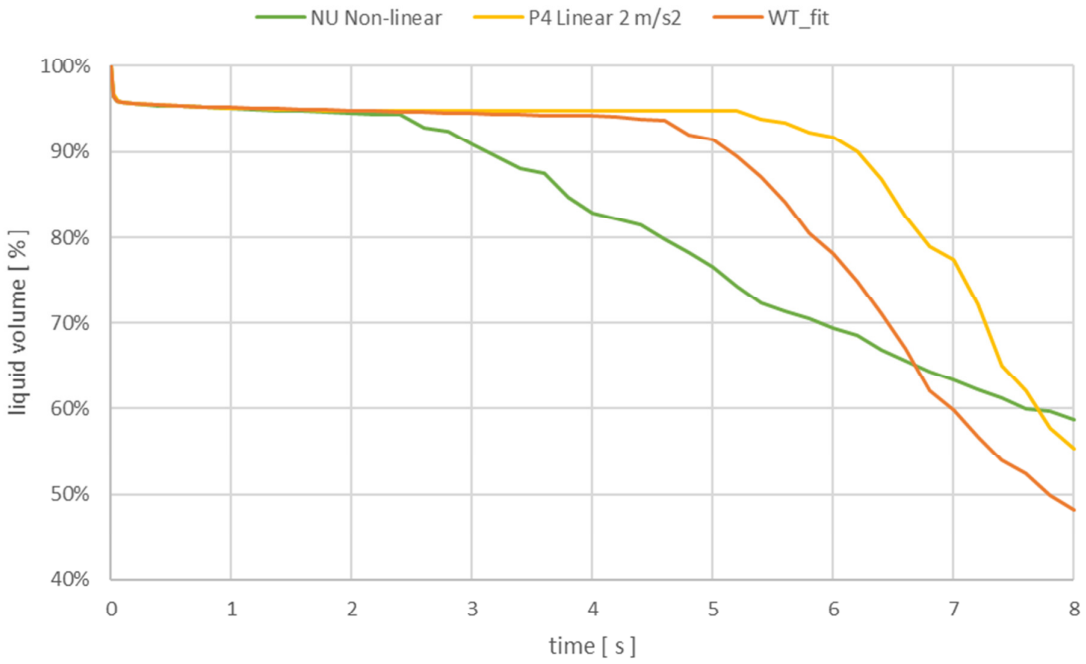

Figure 8. Total liquid volume % on the flat plate over time for cases NU, P4, and WT_fit.

The rate of the liquid removal can already be approximated from Figure 8 by looking at the slopes of the curves, but it is also shown as moving average over 1 second in Figure 9. The highest rate is observed in case P4 which happens probably due to formation of a larger waves causing bigger drops in volume as they exit the domain.

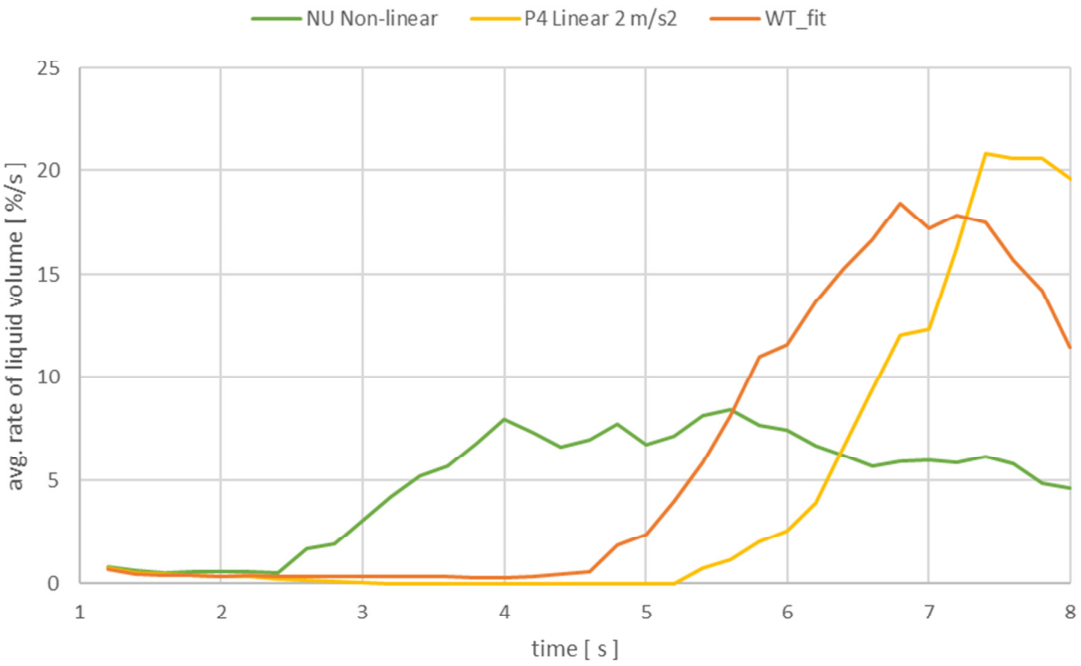

Figure 9. Liquid volume flow rate %/s averaged over 1 second (moving average).

The results of case NU have been reported in ref. [1]Honkanen and Koivisto up to 5 seconds of simulated time. Since the liquid removal over time is clearly different compared to cases P4 and WT_fit, case NU is omitted from further comparison. Results from cases P4 and WT_fit and the inflow velocities are compared with wind tunnel results in Figure 10. Obviously, the velocity of the case WT_fit matches with the wind tunnel velocity since it is fitted. This is not the case with P4 where a timeshift must be used in order to compare the results with same instantaneous inflow velocity rather than simulated time. This is done in Figure 11 where the P4 results have been shifted -2.5 seconds to approximately match the inflow velocity. The agreement of the liquid volume with wind tunnel results is reasonably good in WT_fit, but not so in P4 regardless of the timeshift.

In order to better compare the simulation results to each other the fluid properties like air density were not changed in case WT_fit. The air density of 1.0 kg/m^3 used in the simulations is different from the wind tunnel tests which is 1.231 kg/m^3. The difference in dynamic pressure is evident in Figure 12. The effect of air density can be compensated with an additional timeshift as explained in ref. [1]Honkanen and Koivisto. This is done in Figure 13 for both cases WT_fit and P4 to match the dynamic pressure.

The agreement of the WT_fit results with the wind tunnel results is good, but for perfect comparison another simulation should be done with the same air density. Also, the effect of the initial velocity condition should still be investigated as this leads to rapid drop in the beginning of the simulations.

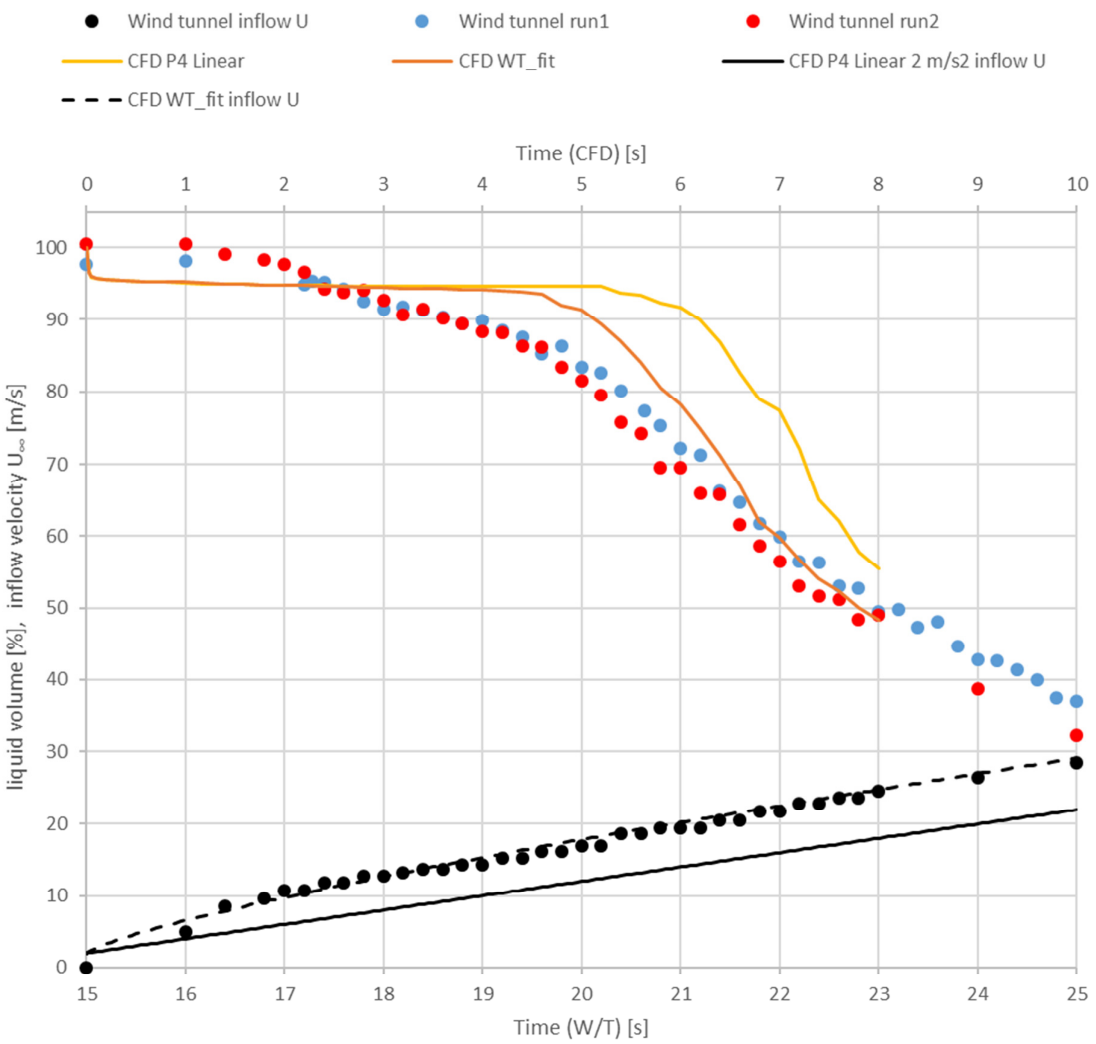

Figure 10. Comparison of the results of cases P4 and WT_fit to the results of wind tunnel runs.

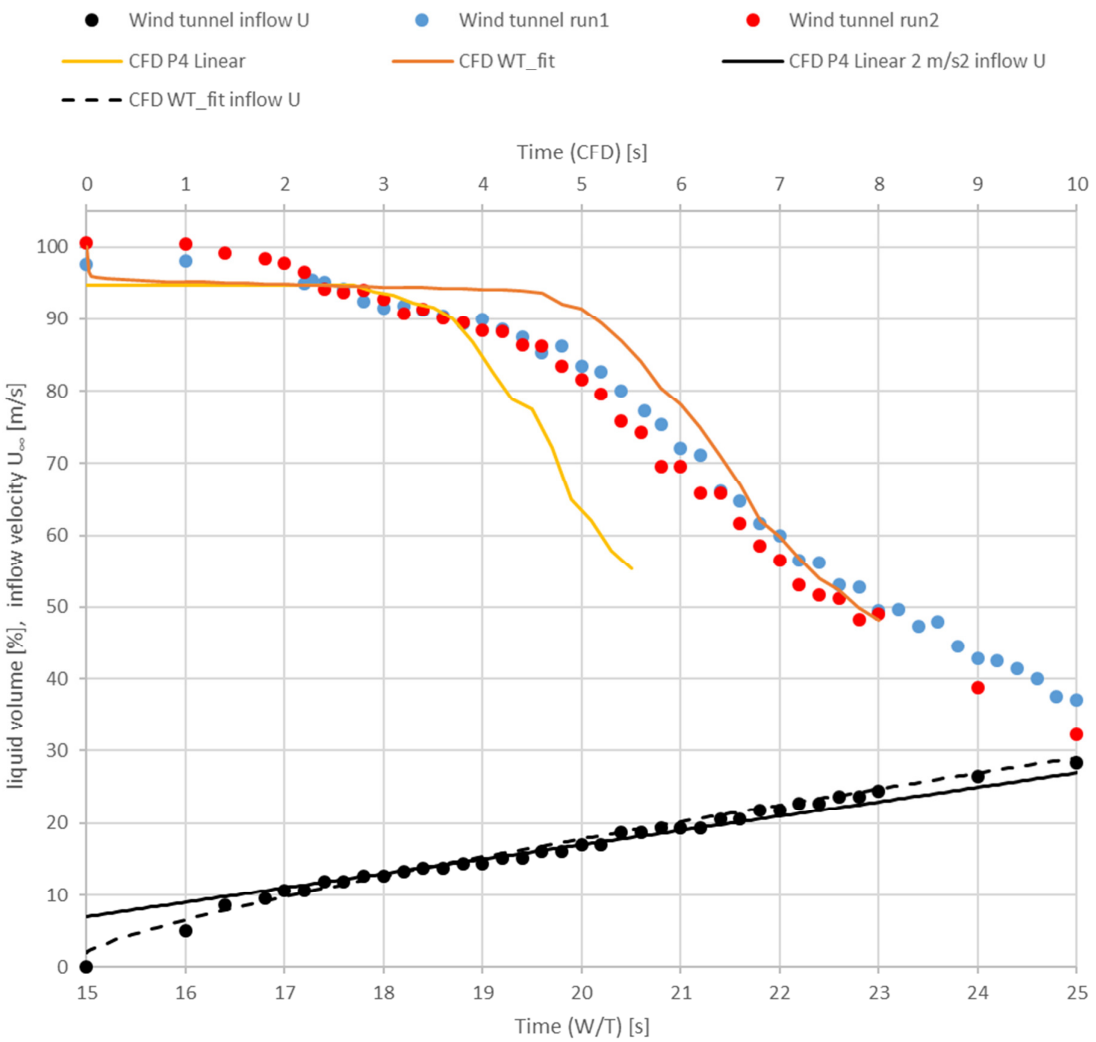

Figure 11. Comparison of the results of cases P4 and WT_fit to the results of wind tunnel runs. The liquid volume result and velocity curves of case P4 have been timeshifted -2.5 s to match the velocity.

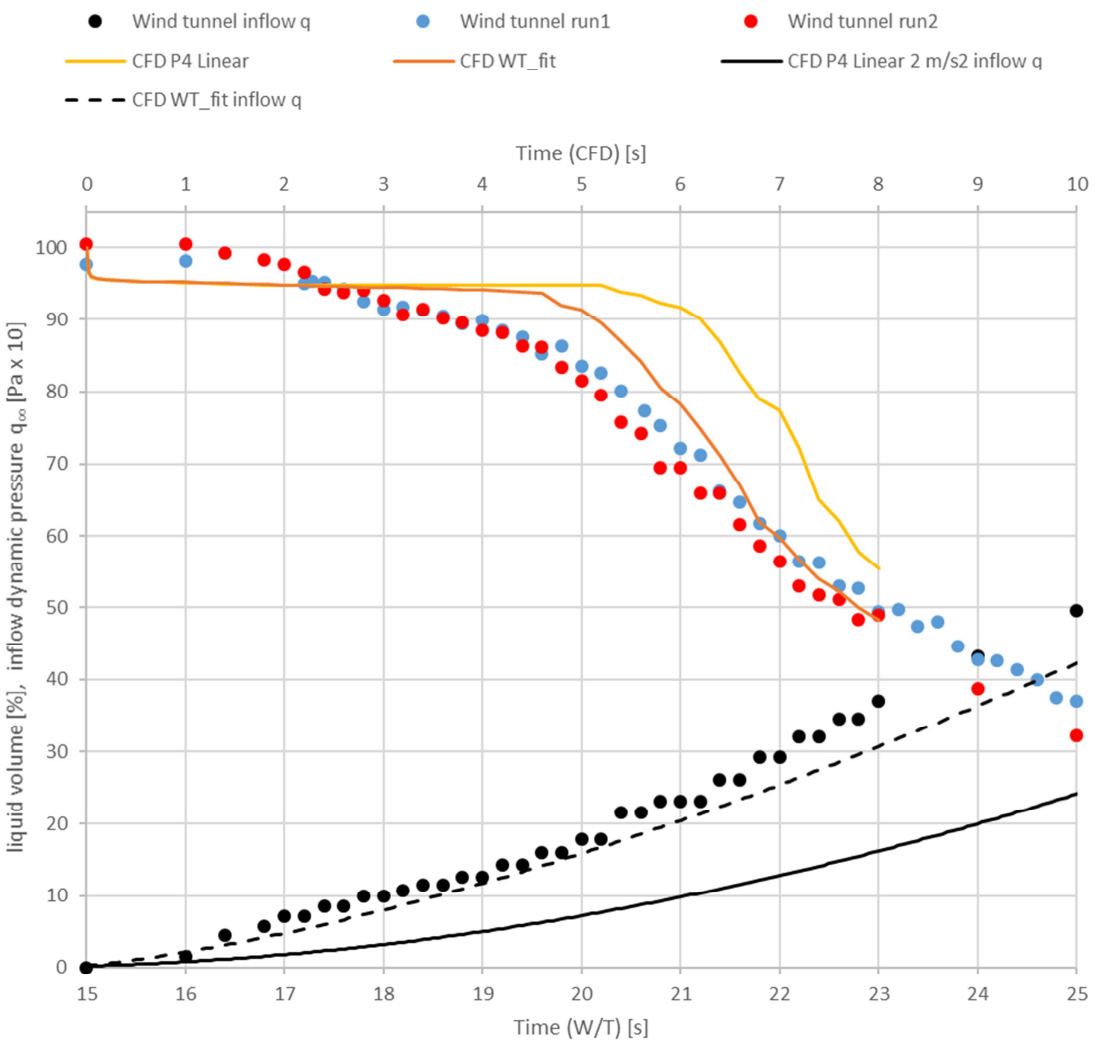

Figure 12. Comparison of the results of cases P4 and WT_fit to the results of wind tunnel runs using the inflow dynamic pressure. The CFD WT_fit inflow q does not match with the Wind tunnel inflow q as the air density is different (1.0 kg/m^3 in CFD, 1.231 kg/m^3 in Wind tunnel).

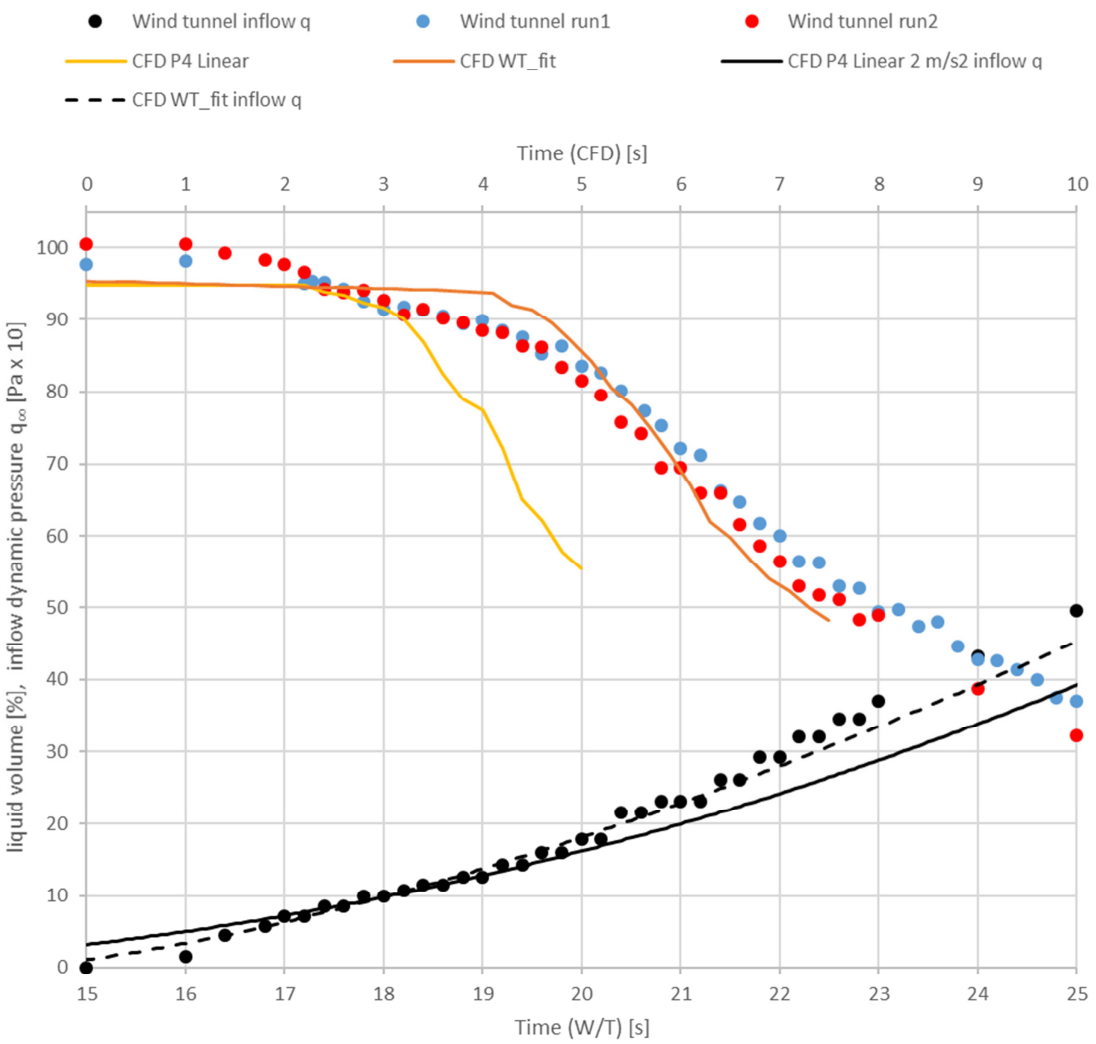

Figure 13. Comparison of the results of cases P4 and WT_fit to the results of wind tunnel runs using the inflow dynamic pressure with timeshift. Case WT_fit and corresponding CFD WT_fit inflow q timeshifted -0.5 s in order to achieve better match to Wind tunnel inflow q, taking into account the difference in air density (1.0 kg/m^3 in CFD, 1.231 kg/m^3 in Wind tunnel). Timeshift for case P4 is -3.0 s.

2.4 Conclusions

The results of the case WT_fit are very good, even though the difference in air density (compared to wind tunnel runs) had to be taken into account with a timeshift. The fitted inflow velocity ramp is the most recommended for future simulations, accompanied with matching fluid properties. However, the computational cost is greater because a longer simulation time is required to reach the point where the liquid removal begins. With the original non-linear velocity ramp of the case NU the removal begins already at approximately t = 2.5 seconds (compared to t = 4 - 5 s with the other cases) because the acceleration is more aggressive as shown in Figure 7.

3 Preliminary testing of non-Newtonian Type IV anti-icing fluid simulation in OpenFOAM

So far the main effort in the Icewing and Frostwing flat plate CFD simulations has been concentrated in simulating Type I deicing fluid. These are Newtonian fluids and therefore viscosity is constant and no additional viscosity modeling is needed. However, wind tunnel tests were also done with the Type IV anti-icing fluid, which is a non-Newtonian fluid. Not all CFD solvers are capable of handling non-Newtonian fluids due to lack of separate viscosity modeling. The presence of the more than one fluid phase in the simulation is another complication, especially if some fluids are Newtonian and others are not. In order to simulate a flow of non-Newtonian fluid on a flat plate and an airflow over it, a quite sophisticated CFD solver must be used.

Fortunately, it turns out that the multiphaseInterFoam solver in OpenFOAM, which has been used in the simulations from the start of the project has the non-Newtonian viscosity modeling capability. A preliminary attempt of non-Newtonian simulation has been made before the wind tunnel measurements using fluid properties obtained from the literature (ref. [3]Koivisto and Auvinen). The viscosity properties of the fluids used in the wind tunnel tests were measured using a viscometer and are different from the values used in the preliminary simulation.

3.1 Power-law viscosity model

In the power-law non-Newtonian viscosity model the instantaneous viscosity of the fluid is computed from the shear rate $S = \partial u/\partial y$ raised to power n-1 and multiplied by constant k as shown in equation (2). The coefficients k and n are obtained from literature, manufacturer data sheets, or measurements.

$$\mu = kS^{n-1} \tag{2}$$

In OpenFOAM code the shear rate used in equation (2) is defined as the magnitude of the symmetric part of the velocity gradient (strain rate tensor) multiplied by $\sqrt{2}$:

$$S = \sqrt{2}\left|\frac{1}{2}\left(\partial_j v_i + \partial_i v_j\right)\right| \tag{3}$$

Additionally, minimum and maximum viscosity values are needed as input in OpenFOAM. Even though the power law model is a well-established viscosity model, it does not model the time dependent effects. The change of viscosity is instantaneous with shear rate while in the real world there is a hysteresis effect which means that if shear rate is removed the viscosity does not rise immediately.

3.2 Type IV anti-icing fluid rheological properties

During the Icewing wind tunnel flat plate tests for the 0.6 meter model, values k = 6100 cP (mPa·s) and n-1 = -0.62 were obtained for the Type IV fluid with the Brookfield viscometer. The maximum viscosity observed during the measurements was 23 000 cP (at 5 °C) and 18 200 cP (at 13 °C). The minimum viscosity was 2250 cP (5 °C) and 2925 cP (13 °C).

In the preliminary non-Newtonian simulation of ref. [3]Koivisto values were taken from ref. [5]Özgen. The simulated fluid was diluted with 75 % water and it was called A25. For this fluid, Özgen gives values k = 168 cP and n-1 = -0.3527.

The A25 fluid from Özgen is considerably less viscous than the 100 % neat Type IV used in the Icewing wind tunnel tests. This is clear from the viscosity vs. shear rate graphs plotted in in Figure 14 using equation (2).

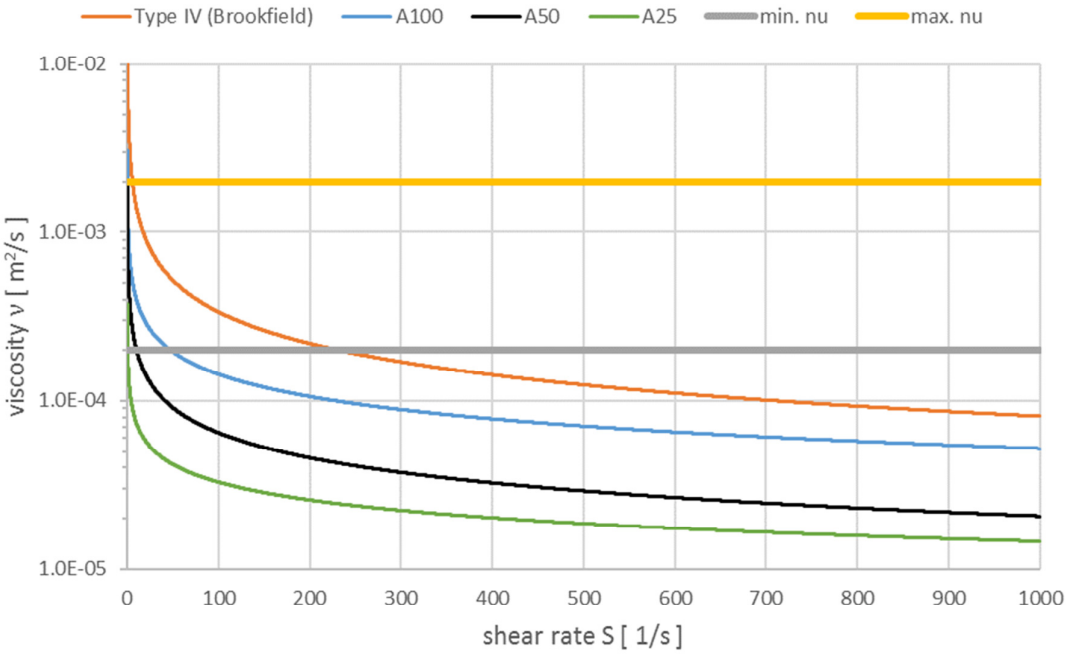

Figure 14. Kinematic viscosity of neat Type IV used in the Icewing wind tunnel tests and different dilutions of the non-Newtonian fluid from ref. [5]Özgen. The minimum (200 cP) and maximum (2000 cP) values are an example to demonstrate the effect of corresponding inputs in OpenFOAM. For example, when S > 200 1/s, the viscosity of Type IV (red curve) will not drop below 2 x 10^{-4} m^2/s (200 cP, grey line).

3.3 Simulation setup and results

The non-Newtonian simulation with the neat Type IV was done with the same type of case setup as most of the previous Newtonian Type I simulations (see ref. [4]Koivisto and Honkanen page 10). The same computational grid with 160 000 cells and flat plate length of 0.6 meters was used with the same non-linear air inflow velocity ramp. The fluid layer initial thickness was 1 mm and the fluid was initially at rest.

Unfortunately, the first simulation failed, producing unphysical results. At first this was thought to be due to the non-Newtonian modeling, but clearly this was not possible because the A25 fluid was successfully simulated as part of the preliminary simulation series before the wind tunnel tests. After looking at the model parameters it was noticed that the viscosity values based on the Brookfield measurements were much higher than the literature based values in the preliminary simulation.

Next, an attempt was made to simulate the same case with the standard Newtonian viscosity model, but with a high viscosity value ν = 2.0 x 10^{-3} m^2/s (2080 cP). This value is 100 times the value used in the Type I fluid simulations and approximately as high as the minimum measured Type IV viscosity. This simulation also failed, showing almost no fluid movement at all. The result looked very similar to the failed non-Newtonian result.

At this point it was reasoned that the problem was either the high value of viscosity, the ν_{liquid}/ν_{air} ratio, or the set maximum and minimum viscosity limits. A limited tri-

al and error effort was started to find a viscosity level which still could be simulated with realistic results.

Further examination of Figure 14 and the problem at hand shows that the minimum and maximum values of the viscosity could be the reason for the unexpected simulation results. In theory, the shear rate S in these simulations could be very high. If the flow speed of the wave crest is 1 m/s and the height of the wave is 1 mm then the shear rate could be in the order 1 m/s / 0.001 m = 1000 1/s, or even higher. This is much higher than is achievable in a Brookfield type viscometer. The procedure of picking the limit viscosity values from the measured Brookfield values is likely incorrect resulting in that the viscosity becomes limited too much (to a high minimum value) when high shear rates are present.

Instead of the A25, the neat fluid A100 was chosen as a reference simulation for the neat Type IV fluid with the Brookfield data. For A100, Özgen gives values k = 1149 cP and n-1 = -0.4422. The viscosity of A100 is still very different from the Type IV as seen in Figure 14. The minimum viscosity value input in the simulations was relaxed and the following cases were simulated for 5 seconds of simulated time:

- A100 (Özgen) ν_{max} = 2.0 x 10^{-3} m^2/s ν_{min} = 2.0 x 10^{-5} m^2/s
- TIV1 (Type IV 100%) ν_{max} = 2.0 x 10^{-2} m^2/s ν_{min} = 2.0 x 10^{-4} m^2/s
- TIV2 (Type IV 100%) ν_{max} = 1.0 x 10^{-2} m^2/s ν_{min} = 2.0 x 10^{-5} m^2/s

The fluid removal over time is shown in Figure 15. It is clear that the fluid removal is minimal during the simulated 5 seconds. The removal of only about 0.4 % is so little, that based on the experience gained with previous simulations with Newtonian fluids it should be neglected. The accuracy of the simulation method depends on the grid resolution. This means that even the formation of the waves could change the volume this much due to the fluid occupying different sized and shaped computational cells.

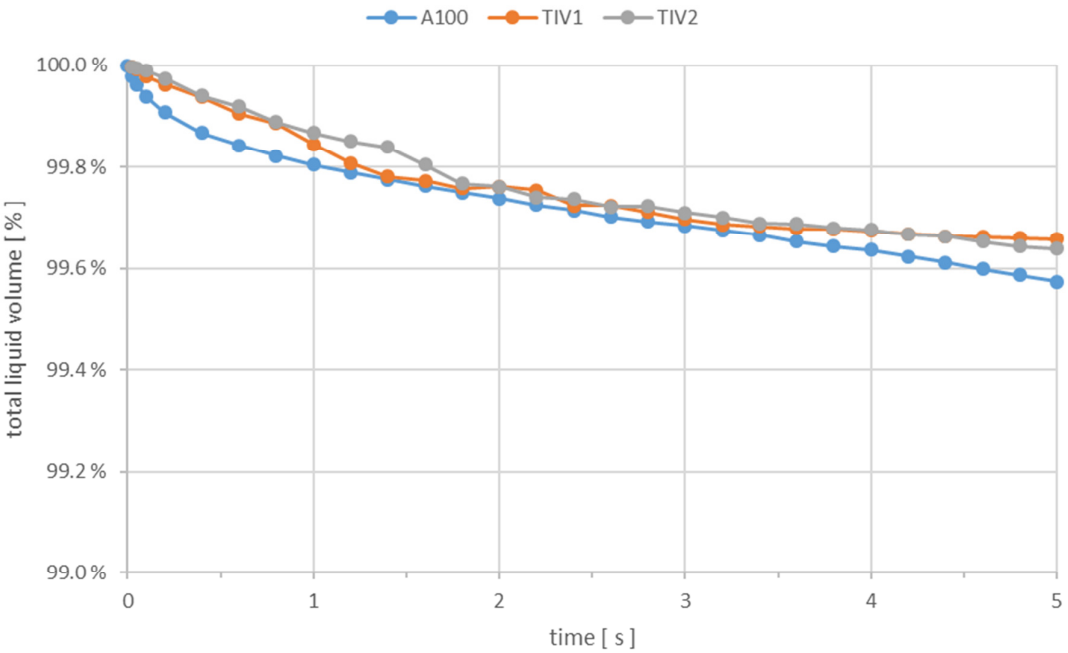

Figure 15. Total fluid volume % on the flat plate over time for cases A100, TIV1, and TIV2.

Even though the differences in the total fluid volume between the cases are negligible, there are qualitative differences in the wave patterns. The wave pattern at t = 1 seconds is distinct in each case as shown in Figure 16.

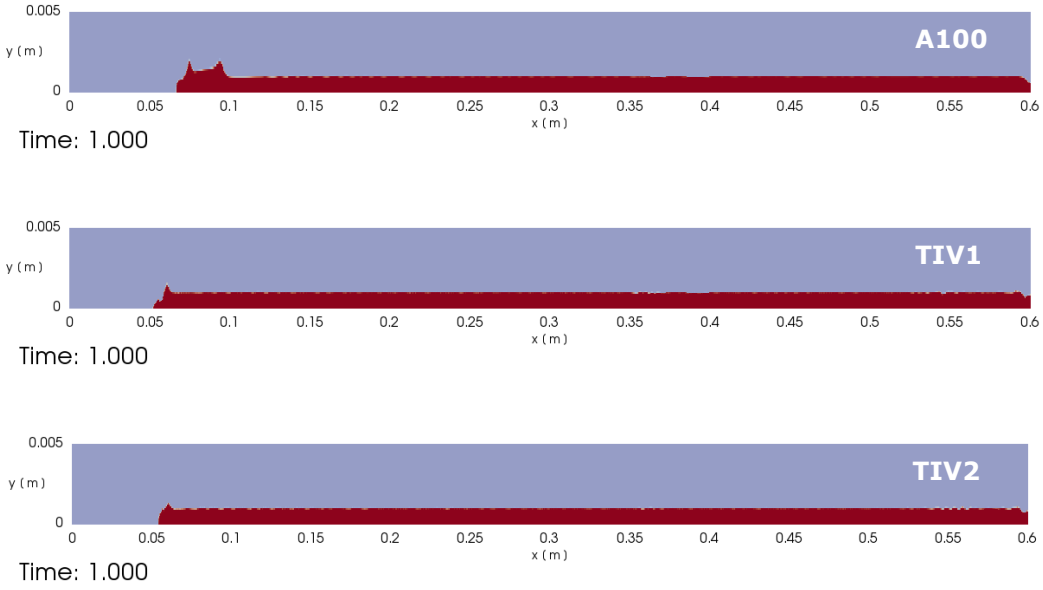

Figure 16. Overview of the fluid interface in cases A100, TIV1, and TIV2 at t = 1 s.

The qualitative differences are even more distinct at the end of the simulations at t = 5 s. This is shown in Figure 17. Now the effect of the viscosity model values (power and coefficient) is visible because the wave pattern in case A100 with lower viscosity is different from cases TIV1 and TIV2. In the case A100 there are waves which move the fluid, but the waves have not reached the trailing edge and hence no removal has yet happened. In the cases TIV1 and TIV2, with the model parameters obtained from the Brookfield test, there are no waves except the deformation of the front edge of the fluid layer. The front edge in TIV1 is different from TIV2 so the change in the minimum and maximum viscosity values does have an effect. The fluid front edge has moved further in TIV2 with lower minimum viscosity limit.

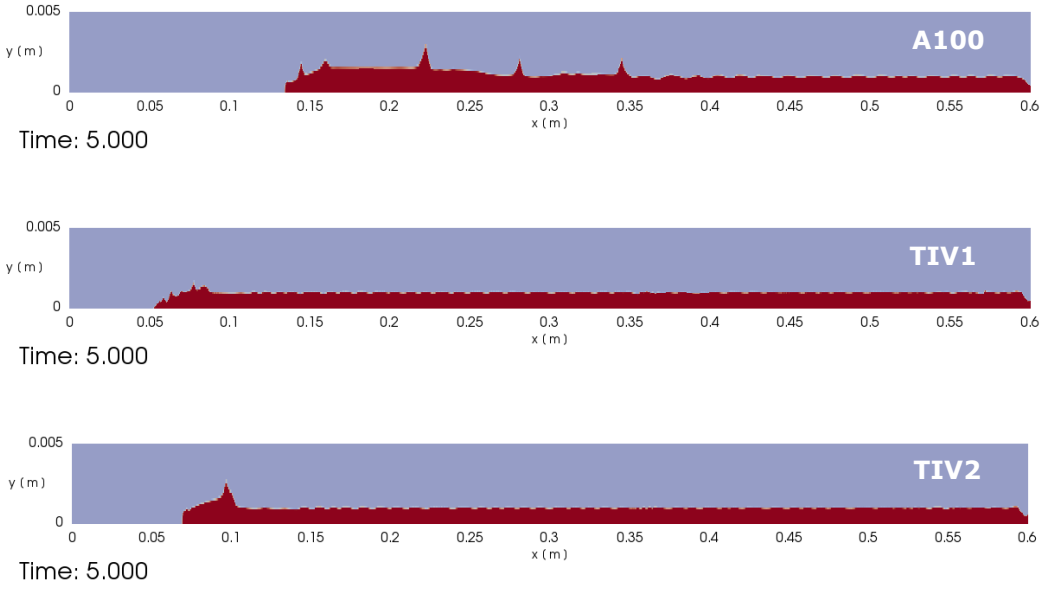

Figure 17. Overview of the fluid interface in cases A100, TIV1, and TIV2 at t = 5 s.

The viscosity distribution of the fluid is shown in Figure 18 at time instant t = 1 s. The minimum and maximum values present at this time instant are shown for each case. It is seen that the maximum limit value is present at some regions or at least some cells in cases A100 and TIV2, which is expected since this follows from zero shear rate. Case TIV1 is different with value 1.124 x 10^{-2} m^2/s. More interesting would be to examine the lowest viscosity but it must be remembered these pictures represent only one time instant and the shear rate and the viscosity could change very rapidly. At least at t = 1 s the minimum viscosity limit is not restrictive in any of the cases sinces the lowest viscosity is higher than the limit. In the case TIV1 the lowest viscosity at this time instant is 3.484 x 10^{-4} m^2/s while the set minimum limit is 2.0 x 10^{-4} m^2/s.

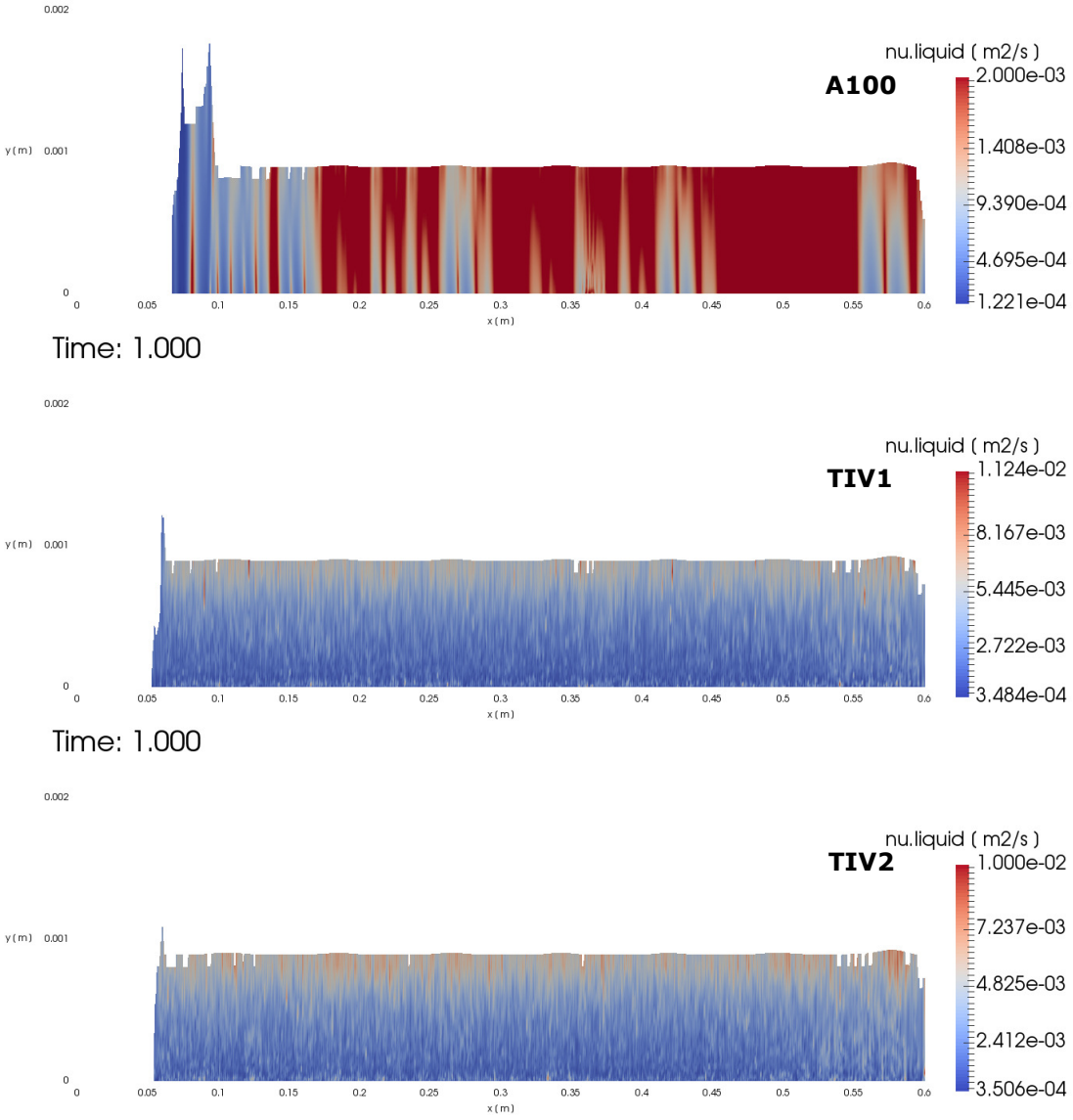

Figure 18. Viscosity distribution (m^2/s) of the fluid in cases A100, TIV1, and TIV2 at t = 1 s.

The viscosity distribution at time instant t = 5 s is shown in Figure 19. Again, when no shear rate is present, the highest viscosity is at the set maximum limit in A100 and TIV2 but not in TIV1. The lowest viscosity at t = 5 s is slightly lower than at t = 1 s in the case A100, but the opposite is true in the cases TIV1 and TIV2 with the more viscous fluid. In these cases the lowest values are higher which suggests that

a lower shear rate is present than at t = 1 s. Clearly these two time instants are insufficient to make any further conclusions about the effect of the minimum viscosity limit values. The simulations should be continued as long as necessary for the fluid removal to begin. One major issue which is obvious from the results is that the fluid removal is much slower compared to the Newtonian Type I simulations where typically about 40 % of the fluid has exited the domain at after 5 seconds of simulated time. In the wind tunnel tests the difference at the fluid removal between Type I and Type IV fluids was small. Therefore, there could still be major limitations in the non-Newtonian modeling and the lack of the hysteresis effect which is present in the real world could be one such limitation.

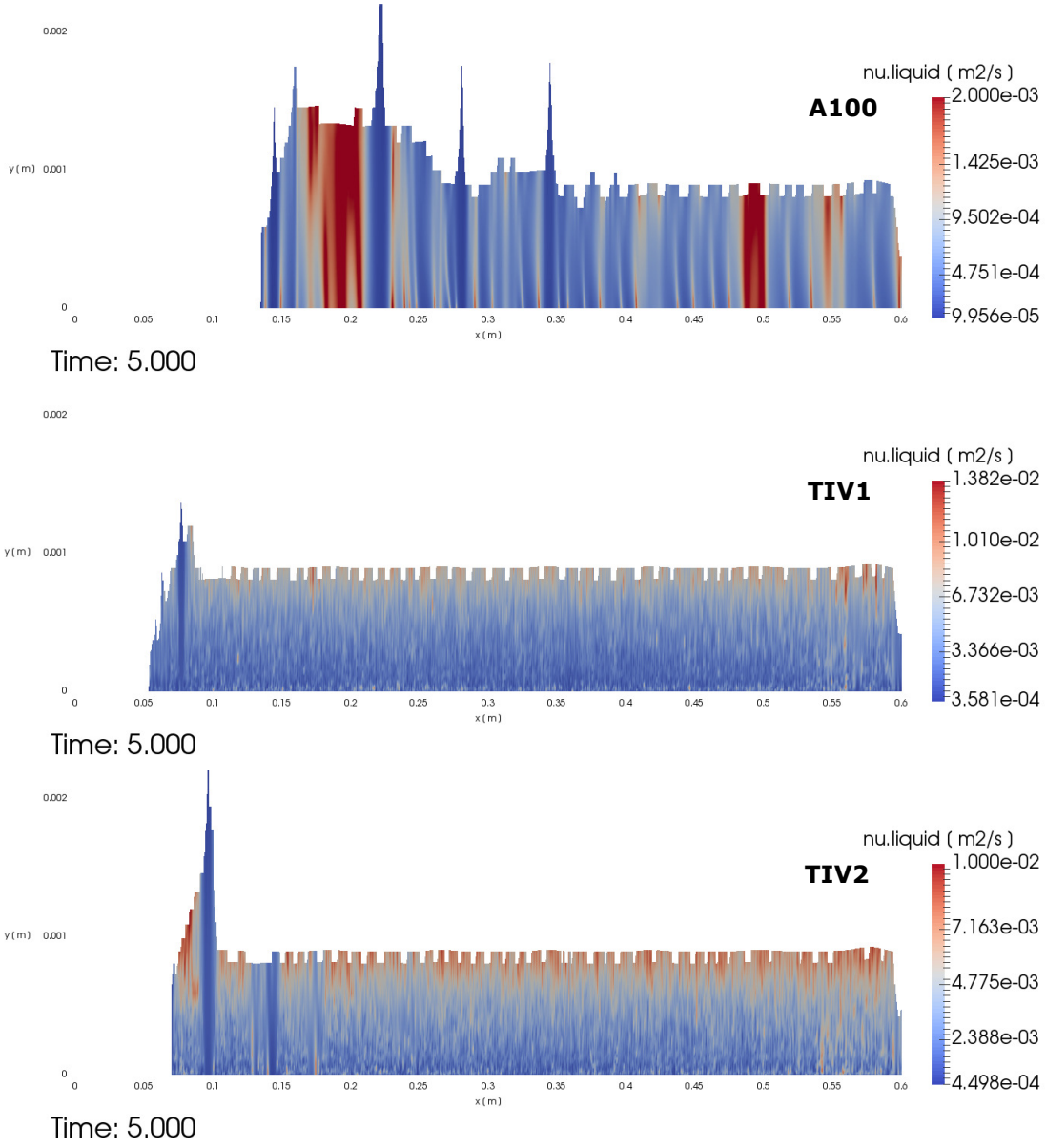

Figure 19. Viscosity distribution (m^2/s) of the fluid in cases A100, TIV1, and TIV2 at t = 5 s.

3.4 A note about the multiphaseEulerFoam solver in OpenFOAM

Another solver option in OpenFOAM that suites multiple fluid phase simulations is the multiphaseEulerFoam solver. However, it has a major limitation in that non-Newtonian viscosity modeling is not supported. This solver has separate momentum equations for each fluid phase. The multiphaseInterFoam solver solves a single momentum equation, and uses a separate mixture code part that uses the volume of fluid (VOF) method to compute the effective fluid properties of the combined mixture by weighing the phase's fluid properties with the phase fraction parameter.

Even though multiphaseEulerFoam does not support non-Newtonian modeling it might be better in handling large differences in the fluid properties. On the other hand, the more detailed Euler-Euler type physics modeling including droplet drag modeling adds new uncertainties. This has been found to be a problem in trials with this solver because droplets separate from the front face of the fluid layer and these flying droplets slow down the computation considerably.

3.5 Conclusions

A preliminary attempt was made to simulate non-Newtonian anti-icing fluids with OpenFOAM solver multiphaseInterFoam. Several problems regarding the simulation setup and the viscous modeling were encountered and relaxing the minimum viscosity limit from the values typically obtained from a Brookfield type viscometer seemed to produce meaningful results.

However, the simulation time of 5 seconds still proved to be insufficient for any quantitative comparison of fluid removal. This also means that the removal process is much slower compared to the Newtonian fluid simulations with the same air acceleration. The removal is also slower to what was observed during the wind tunnel tests. In the wind tunnel the removal rate did not change much between Newtonian Type I and non-Newtonian Type IV fluids. The lack of time effect or hysteresis modeling in the simulation could be a factor. With the current model the changes in local viscosity are instantaneous with shear rate. Also, the grid resolution could affect the situation because ultimately the viscous distribution is discrete and there could be large gradients from cell to cell. This is visible by carefully examining Figures 18 and 19. If further effort is put in the non-Newtonian simulations, the next step should be to continue the simulations until the waves reach the trailing edge of the flat plate and the fluid removal begins.

References

[1]Honkanen T. and Koivisto P., The effect of the air density on the flat plate CFD results, Arteform memorandum, 7 Nov 2016, 7 p.

[2]Honkanen T., Post-processed results of the Icewing 3 preliminary flat plate CFD simulation series, Arteform memorandum, 20 Jul 2016, 26 p.

[3]Koivisto P. and Auvinen M., Preliminary CFD Investigation of De/anti-icing Fluid Behavior on a Flat Plate, Trafi Research Report 5/2015, 2015, 18 p.

[4]Koivisto P. and Honkanen T., Grid Resolution and Parameter Sensitivity Study of Flat Plate CFD Simulations, Trafi Research Report 4/2016, 2016, 42 p.

[5]Özgen S., Carbonaro M., Sarma G.S.R., Experimental study of wave characteristics on a thin layer of de/anti-icing fluid, Phys. Fluids, Vol 14, No 10, October 2002